



# Designing regression approach for mode frequency prediction of empty and filled steel silos

Aashish Kumar Jain<sup>a</sup>, Rajesh Bhargava<sup>b</sup>, Aruna Rawat<sup>a,\*</sup>

<sup>a</sup> Department of Civil Engineering, University Institute of Technology (UIT), Rajiv Gandhi Proudyogiki Vishwavidyalaya (RGPV), Bhopal, 462 033, Madhya Pradesh, India

<sup>b</sup> RGPV, Bhopal, 462 033, Madhya Pradesh, India

## ARTICLE INFO

### Keywords:

Regression  
Aspect ratios  
Closure  
Free vibration  
Mode shape  
Silo  
Thin cylindrical shell

## ABSTRACT

In this study the primary objective is to design prediction model for the free vibration analysis of thin circular cylindrical steel silos having various aspect ratios in empty and varying filled conditions for different types of closures. A finite element method (FEM) is used to carry out the free vibration analysis of steel silos. It is found that the effect of different aspect ratios slender, intermediate slender and squat steel silos is very significant for dynamic response of silo. The silos are considered having open, flat and cone type of closures at its top end. The clamped-free (cantilever) boundary condition is taken for this approach as actual silos are fixed at flat-base. The structural mass of thin cylindrical shell steel silo is made constant for a particular height and diameter. The eigenvalues of the thin cylindrical shell steel silos are extracted by using block Lanczos method. The free vibrations of thin cylindrical shell steel silo with different aspect ratios, radius to thickness ratio are studied. From the present studies it is seen that as aspect ratio increases the fundamental frequency is reduced in empty silo. It is more in the case of squat silo. It can be seen that the fundamental frequency is less in the case of flat closure in all the aspect ratios of the silo. The frequency values are more in the case of cone closure is observed. Also as the mode number increases the modal frequency value increases. Further, as the filling level is increased the modal frequency also increases. Finally, regression approach is adopted for predicting the mode frequency of empty and filled silos for wide range of aspect ratios.

## 1. Introduction

The cylindrical steel silos are constructed with most common circular shell structures. The silos are used for storing, handling and transportation huge quantity of solid materials like cement, grains, fly ash, carbon black, coal saw dust etc. in industrial sector. The storage capacity of tall structures, which are circular in shape and intended for storing huge quantity of material, is in axial direction [1,2]. The plane of rupture at silo start from bottom edge of bins intersects the surrounding wall of silo. The main challenge in analyzing silos is that the mass of silo is comparatively lower than the storage material mass and also the granular nature of storage material. A specific procedure has to be adopted in filling and emptying the silos otherwise it affects the overall stability and dynamic behavior of silo [3]. reviewed the various reasons for damage and failures of silos in the past. The challenge also lies in studying the dynamic interaction behavior between the storage materials and walls or base of silo. Although much progress has been made, some

\* Corresponding author.

E-mail addresses: [jain.aashish0@gmail.com](mailto:jain.aashish0@gmail.com) (A.K. Jain), [rajeshbhargava.bpl@gmail.com](mailto:rajeshbhargava.bpl@gmail.com) (R. Bhargava), [rawataruna14@gmail.com](mailto:rawataruna14@gmail.com) (A. Rawat).

## Nomenclature

3-D	Three-dimensional
ANFIS	Adjustable Neurofuzzy Fuzzy
ANN	Artificial Neural Network
C-C	Clamped-Clamped
C-F	Clamped-Free
CFST	Concrete-Filled Steel Tubular
DEM	Discrete Element Modeling
DM	Donnell-Mushtari
FE	Finite Element
FEM	Finite Element Method
FLH	Flügge
ML	Machine Learning
R <sup>2</sup>	Coefficient of determination
RCGA	Real Coded Genetic Algorithm
RMS	Root Mean Squared Error

aspects of free vibration examination of silo are still lacking, as it is the basic stage in its dynamic design, as it considers both the effective mass contributing to the dynamic response and the stiffness of the silo wall.

The standard on actions on steel structure using EN 1991-4 classifies silos solely on the basis of their aspect ratio (height over diameter,  $H/D$ ) [4]. The different types of silo on the basis of height to diameter aspect ratio are classified as slender silo ( $H/D > 2.0$ ), intermediate slender silo ( $H/D = 1.0$  to  $2.0$ ) and squat silo ( $H/D = 0.4$  to  $1.0$ ), where,  $H$  = height of the cylindrical silo and  $D$  = diameter of cylindrical silo. In practice, cylindrical steel silos are constructed with closure (covering at the top) to protect the stored materials from environment. The closures are attached to the top peripheral edge of the silo wall mainly having the shape of flat, hemispherical, torispherical, ellipsoidal, conical and toriconical. The mass of closures and bulking materials affects the dynamic characteristics of the silo.

Brief reviews of past researchers carried out on silo and vibration of cylindrical shell are presented hereafter [5]: analyzed the effect of earthquake ground motion on the behavior of flat-bottom silo walls [6]. presented static and dynamic silo loads using finite element models. The parameters such as dilatancy angle and Poisson ratio which exert a great influence on lateral pressures exerted on silo walls were taken into account [4]. investigated the validity of the conservation of the design process for metal silos of different aspect ratios range  $0.65 \leq H/D \leq 5.20$  designed according to the EN 1993-1-6 and EN 1993-4-1. They also explored the behavior of five thin-walled cylindrical silos with stepwise-varying wall thickness using finite element method [7]. compared the results obtained by conducting experimental studies on cylindrical silo with those using a finite element model [8]. studied the influence of thickness of shell on the buckling behavior of a typical steel silo under earthquake loads [9]. estimated the fundamental period of vibration of flat-bottom circular silos and compared the results with the experimental fundamental frequencies of silo [10]. studied the effect of different boundary conditions on single-walled carbon nanotube vibrations for the armchair type using wave propagation method [2]. investigated the dynamic buckling behavior of steel silos having different slenderness ratio subjected to horizontal base excitations [11]. investigated the vibrations of functionally graded rotating single-walled carbon nanotubes (SWCNT) with ring supports attached in the radial direction. The impacts of revolving armchairs, zigzag SWCNTs with ring supports, and length- and height-to-radius ratios were thoroughly examined. It was found that for boundary conditions clamped-clamped (C-C) and clamped-free (C-F), increasing length- and thickness-to-radius ratios results in decreasing and rising frequency behaviors, respectively.

[12] carried out a thorough survey of the most notable experimental and theoretical developments related to the dynamic and seismic behavior of flat-bottom cylindrical silos [13]. carried out the experimental studies to determine strain curve, axial load-displacement curve, critical buckling load and also buckling modes under localized axial compression load of steel cylindrical shells [14]. determined the frequencies of single-walled carbon nanotubes using Kelvin's method. For these tubes, thorough investigations of the effects of frequencies on length-to-diameter ratios with varied power law indices were conducted. Also, Hussain and Naeem [15] studied the effect of mass density on vibration of zigzag and chiral SWCNT. It was observed that by increasing values of in-plane rigidity, resulting frequencies also increase and frequencies decrease on increasing mass density per unit lateral area. Moreover [16], adopted Sander's thin shell theory to analyze the frequency analysis of zigzag FG-CNTs with ring-stiffeners. The frequency equation had been extracted using the Ritz approach. Further, Hussain and Naeem (2019b)[17] analyzed the vibration of zigzag and chiral rotating functionally graded carbon nanotubes using wave propagation method [18]. studied the structural behavior, vulnerability, and risk of industrial silos focused on the content and container interaction [19]. studied the vibration of rotating cylindrical shell using polynomial, exponential and trigonometric volume fraction laws. The functionally graded materials steel and nickel along the shell radius direction were considered. These findings show that the shell frequency was split into two halves, and it was inferred that the backward frequency value was somewhat greater than the forward frequency.

[20] determined the vibration of functionally graded (FG) rotating cylindrical shell with ring supports along the circumferential direction using Galerkin's technique. The resultant backward and forward frequencies rise with rising ranged values of the height-to-radius ratio, whereas frequencies decrease with increasing length-to-radius ratio. For various ring support positions,

bell-shaped type of frequencies was observed. Further, it was also observed that as the rotating speed increases, the backward frequencies rises and forward frequencies falls [21]. estimated the vibration frequencies of laminated composite cylindrical shell using Love's shell theory.

[22] determined the vibration coupled and uncoupled frequencies of fluid-filled (non-viscous) three-layered FG cylindrical shells. It was found that as the circumferential wave mode increases, the frequency values also increases. The changes in frequencies are higher under clamped-clamped situations than they were under other boundary conditions. The frequencies are noticeably reduced in case of cylindrical shell with fluid effect. Hussain and Selmi [23] carried out the vibration analyses of shell supported by ring around its circumferential using Rayleigh-Ritz formulation. From the results it was found that clamped-clamped, simply supported-simply supported frequency curves were higher than clamped-simply boundary condition [24]. presented the orthotropic vibration analyses of single-walled carbon nanotubes. It had been shown that raising the aspect ratio raises the frequencies while increasing the nonlocal parameter reduces them, making the clamped-free frequencies lower than those of the clamped-clamped calculation.

The structural and seismic responses and the several uncertainties in the design and assessment processes were also examined. The free vibration analysis of empty and different filled levels of silo along with different closures is examined in the present work. This investigation will definitely results in the understanding the structural and dynamic response of steel silos, also the dynamic interaction behavior between the storage materials and the structural components of flat-bottom silo.

1.1. Review of regression approaches

Recently [25], covered gap in the literature by effectiveness ML (machine learning) algorithms to estimate the shear strength of short links. ML algorithms have been effectively applied in many structural engineering disciplines. They have used artificial neural network (ANN) based shear strength forecasting. A combined machine learning (ML) methodology by Le [26] was put forth to forecast axial load carrying capacity of ellipsoidal CFST columns. The Adjustable Neurofuzzy Fuzzy based (ANFIS) and Real Coded Genetic Algorithm (RCGA) were the suggested models, but these models required large database as inputs for features extraction [18]. presented the potential mechanisms of failure indicated either by materials stored and also the targeted structural configuration, as well as risk assessment and mitigation techniques [27]. described a process for creating and validating metamodels based on DEMs (discrete element modeling). Include a case study of a releasing hopper to show how metamodels and DEMs work together. For three various metamodels that were learned using DEM data and it was also demonstrated that use of polynomial regression for evaluation and

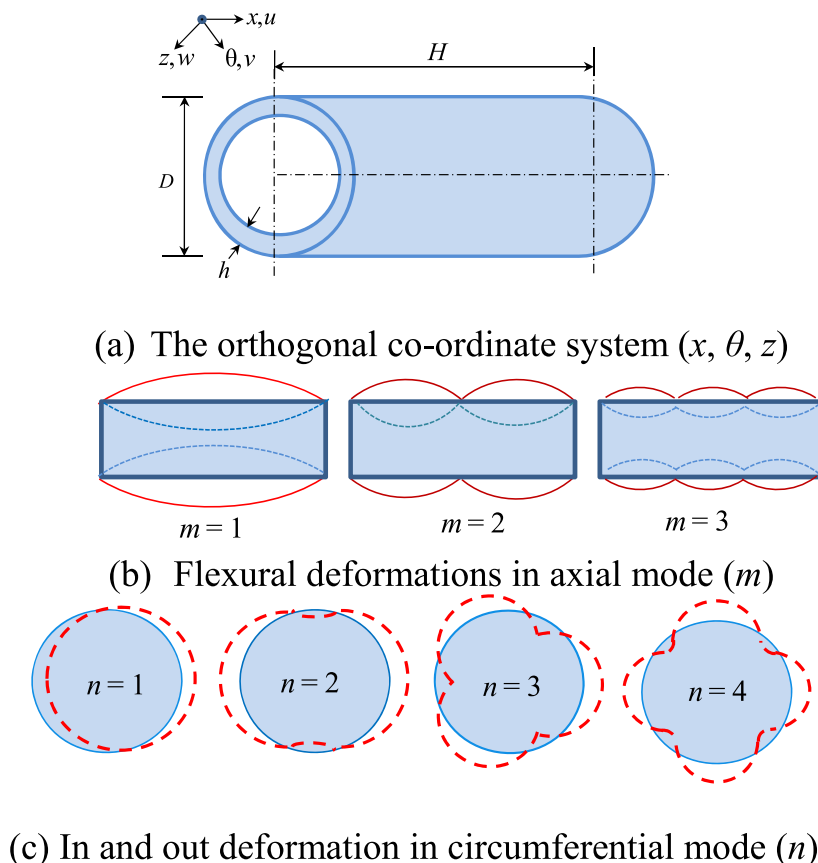


Fig. 1. Different modes in circular cylindrical shell.

prediction of silos design parameters. This is a motivation to adopt regression technique in the present study.

### 2. Contribution of work

Accordingly the main objectives of the present work are to carry out the free vibration analysis of thin circular cylindrical steel silos having various aspect ratios, slender, intermediate slender and squat silos; in empty and varying bulking material filled conditions. The modal frequencies of empty and for 25 %, 50 %, 75 and 90 % filled silos are evaluated. Also, silos are considered having open, flat and cone type of closures at its top, in order to study the effect of closures on the natural frequencies of silos. The clamped-free (cantilever) boundary condition is taken for this approach as actual silos are fixed at flat-base. The eigenvalues of the thin cylindrical shell steel silos are extracted by using block Lanczos iteration method. This paper aimed to design mathematical learning based fundamental mode frequency prediction model for such silos. Regression approach is adopted for predicting the model for mode frequency of empty and 90 % filled silos which allow us to predict for any case of aspect ratio. Mode frequency of empty and 90 % filled silos determined from FEM analyses are used to train the generalized polynomial fitting based prediction model.

However, there are some additional factors that can affect the modal frequency of cylindrical steel silos such as geometrical imperfection, varying wall thickness along the height of silo, stiffener arrangements, and also various properties of bulking materials. Furthermore, three steel silos are examined in the present work, taking into account a larger variety of heights and diameters, different filling levels and also type of closures can improve the accuracy of the assessments reached on the aspect ratios, filling levels and types of closures of the silos.

### 3. Mathematical formulation

Many researchers in past [28–38] carried out the free vibration analysis of shell elements. A circular cylindrical shell is considered having constant thickness ( $h$ ); diameter ( $D$ ); and height (or length), ( $H$ ) with material properties as density ( $\rho$ ); Poisson’s ratio ( $\nu$ ) and modulus of elasticity ( $E$ ). At mid surface of the shell, the co-ordinate system ( $x, \theta, z$ ) is considered and the corresponding axial displacement in  $x$  direction is denoted by  $u(x, \theta, t)$ , circumferential displacement in  $\theta$  direction is  $v(x, \theta, t)$  and radial displacement in  $z$  direction is  $w(x, \theta, t)$  as shown in Fig. 1(a). The circular cylindrical shell vibrates in flexural deformations in axial mode ( $m$ ) along  $x$  direction as shown in Fig. 1(b); in and out deformation in the form of cosine waves,  $\cos(n\theta)$  in circumferential mode ( $n$ ) along  $\theta$  direction as shown in Fig. 1(c) and radial mode is ignored due to axi-symmetry condition of the shell. Accordingly, any combination of axial and circumferential ( $m, n$ ) modes defines the vibrational modes and the related modal frequencies of the circular cylindrical shell.

In case of free vibration of cylindrical shell, when the external forces are absent, the equations of motion are given as [39].

$$\frac{Eh}{1-\nu^2} \left( \frac{\partial^2 u}{\partial x^2} + \frac{1-\nu}{2R} \frac{\partial^2 u}{\partial \theta^2} + \frac{\nu}{R} \frac{\partial w}{\partial x} + \frac{1+\nu}{2R} \frac{\partial^2 v}{\partial x \partial \theta} \right) = \rho h \ddot{u} \tag{1}$$

$$\frac{Eh}{1-\nu^2} \left( \frac{1-\nu}{2} \frac{\partial^2 v}{\partial x^2} + \frac{1}{R^2} \frac{\partial^2 v}{\partial \theta^2} + \frac{1}{R^2} \frac{\partial w}{\partial \theta} + \frac{1+\nu}{2R} \frac{\partial^2 u}{\partial x \partial \theta} \right) + \frac{D}{R^2} \left( \frac{1-\nu}{2} \frac{\partial^2 v}{\partial x^2} + \frac{1}{R^2} \frac{\partial^2 v}{\partial \theta^2} - \frac{1}{R^2} \frac{\partial^3 w}{\partial \theta^3} - \frac{\partial^3 w}{\partial x^2 \partial \theta} \right) = \rho h \ddot{v} \tag{2}$$

$$\frac{Eh}{1-\nu^2} \left( -\frac{1}{R^2} \frac{\partial v}{\partial \theta} - \frac{w}{R^2} - \frac{\nu}{R} \frac{\partial u}{\partial \theta} \right) + \frac{D}{R^2} \left( -R^2 \frac{\partial^4 w}{\partial x^4} + \frac{\partial^3 v}{\partial x^2 \partial \theta} - 2 \frac{\partial^4 w}{\partial x^2 \partial \theta^2} - \frac{1}{R^2} \frac{\partial^4 w}{\partial \theta^4} + \frac{1}{R^2} \frac{\partial^3 v}{\partial \theta^3} \right) = \rho h \ddot{w} \tag{3}$$

where  $D = Eh^3/12(1 - \nu^2)$  is bending stiffness/flexural rigidity

The equations of motion in matrix form for the free vibration of a cylindrical shell as proposed by Refs. [40,41] is given as

$$\begin{bmatrix} L_{11} & L_{12} & L_{13} \\ L_{21} & L_{22} & L_{23} \\ L_{31} & L_{32} & L_{33} \end{bmatrix} \begin{Bmatrix} u(x, \theta, t) \\ v(x, \theta, t) \\ w(x, \theta, t) \end{Bmatrix} = \begin{Bmatrix} 0 \\ 0 \\ 0 \end{Bmatrix} \tag{4}$$

where differential operators with respect to  $x, \theta$ , and  $t$  is  $L_{ij}$  ( $i, j = 1, 2, 3$ ). The vibration behavior of circular cylindrical shells is modeled using several systems of equations [42]. A synchronous motion is assumed in the initial effort to solve the governing differential Equation (1).

$$\begin{aligned} u(x, \theta, t) &= U(x, \theta) f(t) \\ v(x, \theta, t) &= V(x, \theta) f(t) \\ w(x, \theta, t) &= W(x, \theta) f(t) \end{aligned} \tag{5}$$

where scalar model coordinate corresponding to the mode shapes  $U(x, \theta), V(x, \theta)$ , and  $W(x, \theta)$  is  $f(t)$ .

The axial, tangential and radial displacements of the shell wall are evaluated using the separation of variables approach so as to distinguish the spatial dependency of the modal shape among axial and circumferential directions

$$\begin{aligned} u(x, \theta, t) &= Ae^{\lambda_m x} \sin(n\theta) \cos(\omega t) \\ v(x, \theta, t) &= Be^{\lambda_m x} \sin(n\theta) \cos(\omega t) \\ w(x, \theta, t) &= Ce^{\lambda_m x} \sin(n\theta) \cos(\omega t) \end{aligned} \tag{6}$$

where  $\omega$  represents angular frequency of free vibration;  $\lambda_m$  represents the axial wave number;  $n$  is the circumferential wave parameter;  $A, B$  and  $C$  represents the undetermined constants. By substituting Equation (6) into Equation (4), a set of homogeneous equations is created. The application of any of the shell theories presented in the aforementioned canonical literature, with the ensuing matrix form,

$$\begin{bmatrix} X_{11} & X_{12} & X_{13} \\ X_{21} & X_{22} & X_{23} \\ X_{31} & X_{32} & X_{33} \end{bmatrix} \begin{Bmatrix} U \\ V \\ W \end{Bmatrix} = \begin{Bmatrix} 0 \\ 0 \\ 0 \end{Bmatrix} \tag{7}$$

where,  $X_{ij}$  ( $i, j = 1, 2, 3$ ) are coefficients and are the functions of frequency parameter,  $\Omega$  is given as  $\Omega^2 = (1 - \nu^2) \rho \omega^2 R^2 / E$  and  $\lambda_m$ , and  $n$ .

The coefficient matrix's determinant must be zero so that in order to get a non-trivial solution,

$$\det([X_{ij}]) = 0, \Rightarrow i, j = 1, 2, 3 \tag{8}$$

By expanding Equation (7), the frequency equation is produced

$$f(\lambda_m, \omega) = 0 \tag{9}$$

For silos are cantilever i.e. clamped-free (C-F) boundary condition is considered, as actual silos are fixed at flat-base. The boundary conditions for the C-F shell are:

$$\begin{aligned} \text{at fixed end : } x = 0 \Rightarrow u = v = w = \partial w / \partial x = 0 \\ \text{at free end : } x = H \Rightarrow M_x = N_x = 0 \end{aligned} \tag{10}$$

where  $M_x$  and  $N_x$  are the axial moment and force in shell, respectively as it deforms. An undamped finite element (FE) model's eigenvalue problem for the modal frequencies is stated as

$$(-\omega^2 M^{mn} + K^{mn}) \Phi^n = 0 \tag{11}$$

where  $M^{mn}$  and  $K^{mn}$  are the mass and stiffness matrices;  $m$  and  $n$  are the degrees-of-freedom;  $\Phi^n$  is the eigenvector (or modes of vibration).

#### 4. Validation of the finite element models

In the present study, finite element method (FEM) is used for the free vibration analysis of cylindrical silo for empty and varying bulking material filled conditions. The block Lanczos iteration methods is used for frequency extraction of the silos. This method is suitable for large symmetrical eigenvalue problems and uses sparse matrix solver [43,44]. This method performs efficiently for FE models consisting of shell element or combined shell and solid elements. The frequency extraction analysis is performed in the FE software ANSYS® [45] using modal analysis. The frequency extraction flowchart is shown in Fig. 2. During the modeling first silo model type is configured, then material properties are assigned to silo model as modulus of elasticity and Poisson's ratio, element types and meshing to model is assigned, clamped-free boundary condition is assigned to silo. The block Lanczos iteration method is

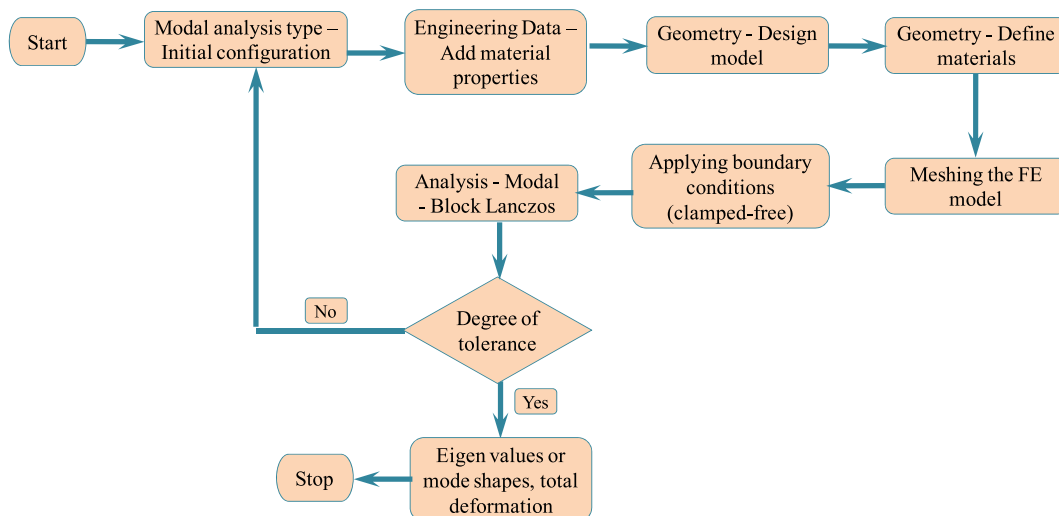


Fig. 2. Flowchart for frequency extraction.

performed until the degree of tolerance for extracting the first twenty modal frequencies. The eigenvalues and mode shapes of silo for different aspect ratio of empty and filled conditions and also for different types of closures are evaluated.

The accuracy of the results obtained from the present FE models has been validated by comparing it with the experimental and analytical results obtained from the past literature results. The results obtained by the present FEM are compared with the experimental results by Sewall and Naumann (1968) and also by published analytical results of Soedel (1980). The parameters for clamped-clamped and clamped-free shell made up of aluminum having parameters:  $R = 242 \text{ mm}$ ,  $H = 625 \text{ mm}$ ,  $h = 0.648 \text{ mm}$ ,  $\rho = 2.7 \times 10^{-9} \text{ N s}^2/\text{mm}^4$ ,  $E = 7 \times 10^4 \text{ N/mm}^2$  and  $\nu = 0.33$ . Fig. 3 shows the modal frequencies ( $f_{mn}$ ) from the present results and that published in the literature for clamped-clamped (C-C) and clamped-free (C-F) boundary conditions. It is observed that the  $f_{mn}$  results obtained from the present FEM are nearly same that obtained from experimental and analysis results. It is also noted that relatively lower values of the frequencies  $f_{mn}$  are obtained for clamped-free case. The lower minimum frequency is achieved for the smaller values of the  $m = 1$ , and as the value of mode number  $m$  increases there is progressive shift in frequencies.

The accuracy of the present FEM is also validated by comparing the results with Lee and Kwak (2015). The modal frequencies obtained were using FE approach in ANSYS® [45] and also compared with Flügge (FLH) and Donnell-Mushtari (DM) theories results. The shell consisting of aluminum having parameters:  $R = 150 \text{ mm}$ ,  $H = 600 \text{ mm}$ ,  $h = 1 \text{ mm}$ ,  $\rho = 2770 \text{ kg/m}^3$ ,  $E = 71 \text{ GPa}$  and  $\nu = 0.33$  is considered. Table 1 shows the modal frequencies ( $f_{mn}$ ) obtained in the present study for C-F boundary condition and the results obtained by Lee and Kwak (2015). It is observed that the modal frequencies results obtained from the present FEM are nearly same that obtained by Lee and Kwak (2015). Moreover, the present FEM is also compared with [22] for without fluid condition of isotropic cylindrical shell material having simply-supported boundary condition. Table 2 shows that present results are in good agreement with [22].

Furthermore, the validation of fundamental frequency of silo filled with bulking material is also verified for the accuracy [2]. determined the fundamental frequencies for slender, intermediate slender and squat silos filled with Camacho wheat as a bulking material. The mechanical properties of wheat are: Angle of internal friction ( $\varphi$ ) = 22.2°, apparent cohesion ( $c$ ) = 0.006 MPa, Coulomb friction coefficient ( $\mu$ ) = 0.19 for steel and 0.42 for concrete, dilatancy angle ( $\psi$ ) = 23.1°, Young’s modulus ( $E$ ) = 10 MPa, Poisson’s ratio ( $\nu$ ) = 0.37, density ( $\rho$ ) = 852.2 kg/m<sup>3</sup>. The geometrical dimensions of silo are described in Table 3. The fundamental frequency obtained from the present study for slender silo is 2.8 Hz, intermediate slender is 3.65 Hz, squat is 3.88 Hz are in acceptable agreement with the frequency predicted by Ref. [2].

### 5. Numerical results and discussions

In the present study, the free vibration analysis of cylindrical steel silo for empty and varying filled conditions of bulking material are evaluated. The eigenvalues are extracted using the block Lanczos iteration method. The cylindrical steel silos slender (S), intermediate slender (I) and squat (Q), for open, flat closure and cone closure are considered as shown in Fig. 4. In order to compare the effect of different aspect ratios, different closure conditions on the free vibration analysis of steel silo. Table 4 presents the parameter of steel silos for different aspect ratios as height to diameter ratio ( $H/D$ ), radius to thickness ratio ( $R/h$ ), thickness to closure thickness ratio ( $h/h_c$ ) for the calculations of modal frequencies. Table also illustrates the storage capacity of each silo type under consideration.

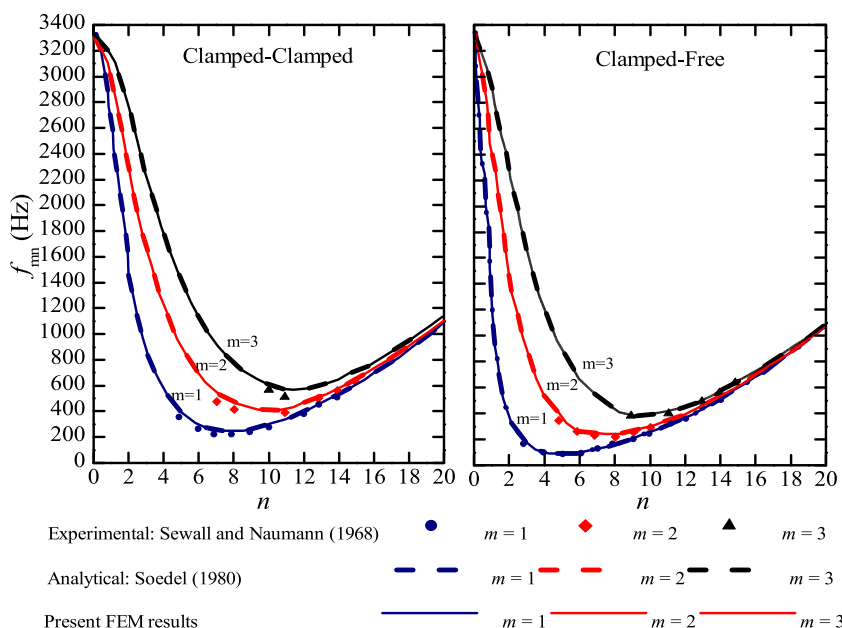


Fig. 3. Natural frequencies of clamped-clamped and clamped-free aluminium shell.

**Table 1**  
Modal frequencies  $f_{mn}$  (Hz) for the present FEM results compared with Lee and Kwak (2015).

Boundary condition	Mode ( $m, n$ )	Present results	ANSYS (Lee and Kwak, 2015)	FLH (Lee and Kwak, 2015)	DM (Lee and Kwak, 2015)
Clamped-Free (C-F)	(1,3)	146	146	146	153
	(1,4)	175	174	175	185
	(1,2)	242	243	242	243
	(1,5)	263	261	263	274
	(1,6)	382	378	381	391
	(2,5)	381	380	381	389

**Table 2**  
Frequencies  $f_{mn}$  (Hz) for the present FEM results compared with [22].

Circumferential wave no. ( $n$ )	Present results	[22] for without fluid condition
1	13.611	13.548
2	4.723	4.592
3	4.368	4.263
4	7.356	7.225
5	11.681	11.542

**Table 3**  
Geometrical dimensions of silos by Ref. [2].

Types of silo	Height ( $H$ ) (m)	Height of silo bulk solids ( $h_b$ ) (m)	Diameter ( $D$ ) (m)	Aspect ratio ( $h_b/D$ )	Thickness ( $t$ ) (mm)
Slender	25	22.5	10	2.25	10
Intermediate slender	18	16.2	12	1.35	8
Squat	12	10.8	15	0.72	6

For the simplicity of the FE model in the present study the thickness of closure ( $h_c$ ) is considered same as the thickness of silo wall ( $h$ ). The angle of cone closure is kept constant  $15^\circ$  with horizontal in all silos. The steel silos are modeled using 4-noded shell 181 element, having six degrees-of-freedom at each node, including rotations about the  $x$ ,  $y$  and  $z$  axes as well as translations in the  $x$ ,  $y$  and  $z$  directions (ANSYS®), with modulus of elasticity ( $E$ ) = 200 GPa, Poisson's ratio ( $\nu$ ) = 0.30, density ( $\rho$ ) = 7850 kg/m<sup>3</sup>. As per EN 1991-4 [46] the boundary condition of silo is a base ring around the circumference of the silo at the base and provides means of attachment of the silo to a foundation or other element. In the present work clamped-free boundary condition is adopted for all silo types.

The slender, intermediate slender and squat silos filled with cement as a bulking material. The material properties of cement are: modulus of elasticity ( $E$ ) = 25 GPa, Poisson's ratio ( $\nu$ ) = 0.20, density ( $\rho$ ) = 1440 kg/m<sup>3</sup>. The bulking material cement is modeled using three-dimensional (3-D) higher order 20-noded solid 186 elements that exhibit quadratic displacement behavior. The element is an isoperimetric brick element defined by 20 nodes with three degrees-of-freedom per node, i.e. translation displacement in nodal  $x$ ,  $y$  and  $z$  directions (ANSYS®). In this work, the surface-to-surface contact mechanism is adopted which defines both the target surface as silo wall and the contact surface as bulking material surface. The interaction between the bulk material and the silo wall is modeled using the Coulomb friction theory. Thus, the coefficient of friction 0.41 is selected between the steel wall and cement. Fig. 5 summarizes the results of the mesh sensitivity analyses based on changing element sizes, based on which 10 mm size of mesh is adopted for the FE model of silos.

### 5.1. Empty silos

Fig. 6 shows the modal frequencies for slender, intermediate slender and squat empty silos, for open, flat closure and cone closure with respect to the mode numbers. The first twenty modal frequencies are extracted from the FE models. For the better understanding of the free vibration of silos, two aspect ratios are considered in case of slender, intermediate slender and squat silos. It can be observed from Fig. 6 (a) and (b) for higher aspect ratios of slender and intermediate slender silos the modal frequencies in cone closure is having higher values. But in case of squat silo in Fig. 6 (c) for lower aspect ratio 0.5 the modal frequencies in cone closure is more. Also it can be seen that as the mode number increases the modal frequency value increases.

Table 5 gives the modal frequencies (in Hz) in empty slender silos. It can be seen that for aspect ratio 2.5 for flat closure the fundamental frequency has reduced by about 50 %, while in cone closure it has increased by around 222 % compared to open silo. As discussed in Fig. 1 description the vibrational modes of circular cylindrical shell are defined by the combination of axial and circumferential ( $m, n$ ) modes. It can be thus seen that in case of slender silo for both aspect ratios for open, flat and cone closures the axial mode in the first three frequencies is the first axial mode while the circumferential modes are categorized by series of cosine waves. But in case of cone closure for frequency mode from fourth mode are having the second axial mode along with the higher order circumferential modes.

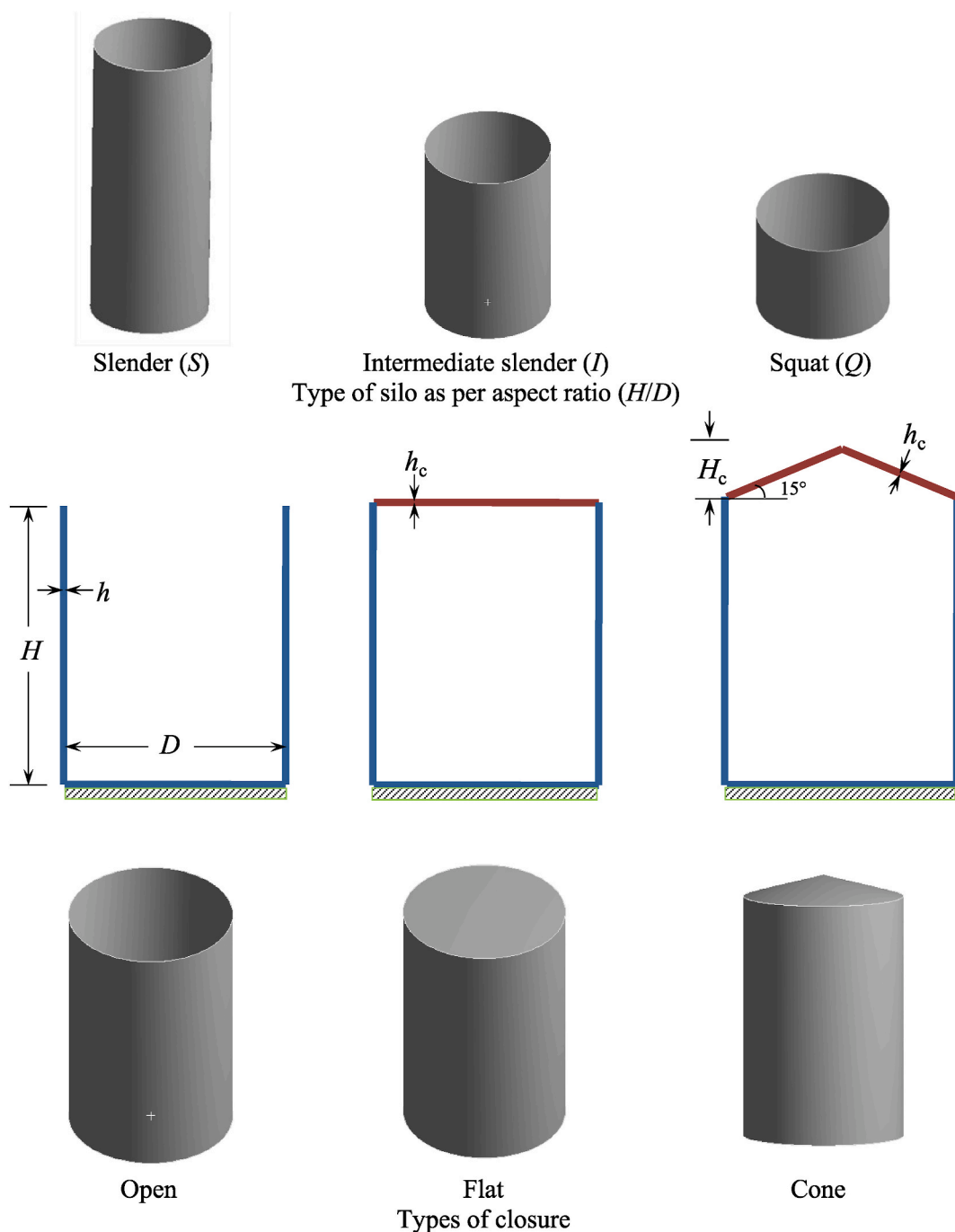


Fig. 4. Cylindrical steel silos.

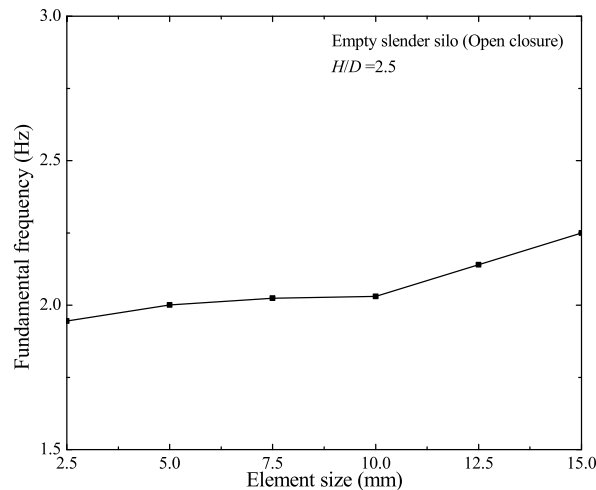
Similarly, Tables 6 and 7 describe the modal frequencies (in Hz) in empty intermediate slender and squat silos, respectively. While the same increment of 216 % is observed for cone closure with the aspect ratio of 2.0. From Table 6 it can be seen that for flat and cone closures for intermediate slender silos the axial mode has increased from 1 to 2 corresponding to aspect ratio of slender silo. It can be observed that in case of intermediate silo for flat and cone closures the frequency modes is a combination of second axial mode along with the series of circumferential modes. And similarly it is also observed in Table 7 in case of cone closure for squat silo the axial mode ( $m$ ) has increased from 1 to 2 due to lesser height of the silo.

As depicted in Table 8 the fundamental frequency in case of slender silo for  $H/D = 2.5$  is 2.03 Hz, 1.01 Hz and 4.51 Hz for open, flat and cone closures, respectively. And for  $H/D = 2.0$  is 1.85 Hz, 0.50 Hz and 4.01 Hz for open, flat and cone closures, respectively. The fundamental frequency in case of intermediate slender silo for  $H/D = 1.5$  is 2.46 Hz, 0.55 Hz and 5.15 Hz for open, flat and cone



**Table 4**  
Parameters of thin cylindrical steel silo.

Type of closure	Type of silo	Height (H) (m)	Diameter (D) (m)	Aspect ratio (H/D)	Thickness (h) (mm)	Radius to thickness ratio (R/h)	Thickness of closure (h <sub>c</sub> ) (mm)	Storage capacity (cum)
Open	Slender (S)	25	10	2.5	10	500	–	1963.495
		20	10	2	5	1000	–	1570.796
	Intermediate slender (I)	18	12	1.5	8	750	–	2035.752
		15	12	1.25	5	1200	–	1696.46
		Squat (Q)	12	15	0.8	6	1250	–
7.5	15		0.5	5	1500	–	1325.359	
Flat	Slender (S)	25	10	2.5	10	500	10	1963.495
		20	10	2	5	1000	5	1570.796
	Intermediate slender (I)	18	12	1.5	8	750	8	2035.752
		15	12	1.25	5	1200	5	1696.46
		Squat (Q)	12	15	0.8	6	1250	6
7.5	15		0.5	5	1500	5	1325.359	
Cone	Slender (S)	25	10	2.5	10	500	10	1963.495
		20	10	2	5	1000	5	1570.796
	Intermediate slender (I)	18	12	1.5	8	750	8	2035.752
		15	12	1.25	5	1200	5	1696.46
		Squat (Q)	12	15	0.8	6	1250	6
7.5	15		0.5	5	1500	5	1325.359	



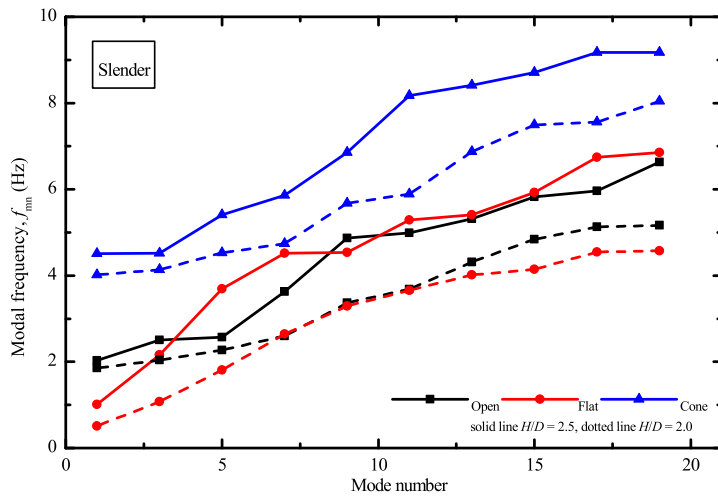
**Fig. 5.** Mesh sensitivity analyses for finite element silo model.

closures, respectively. And for  $H/D = 1.25$  is 2.33 Hz, 0.35 Hz and 5.04 Hz for open, flat and cone closures, respectively. Further, the fundamental frequency in case of squat silo for  $H/D = 0.8$  is 2.90 Hz, 0 Hz and 6.15 Hz for open, flat and cone closures, respectively. And for  $H/D = 0.5$  is 4.29 Hz, 0.22 Hz and 6.88 Hz for open, flat and cone closures, respectively. It can be observed that as the aspect ratio increases the fundamental frequency is reduced in empty silo. It is more in the case of squat silo. As frequency is inversely proportional to mass of silo, thus in case of slender silo as the dimensions of silo are increased, the mass of silo increases, owing to decreased frequency values. The effects of flat and cone closures on the frequency of silo is also investigated in the present study. It can be seen that the fundamental frequency is less in the case of flat closure in all the aspect ratios of the silo. The frequency values are more in the case of cone closure silo. From the geometry of open, flat closure and cone closure the height and the mass is more in case of cone closure, thus increases the mass of empty silo and lessens the frequency values.

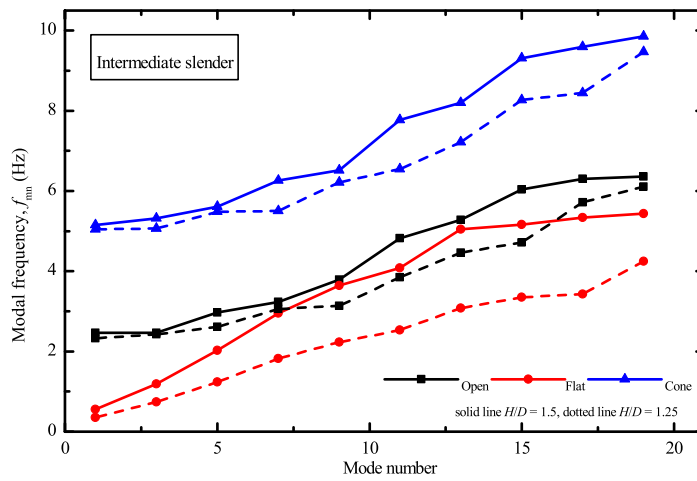
5.2. Different filling levels of silos

The effect of varying cement filled condition in silo on the modal frequencies is also investigated. Fig. 7 shows the modal frequencies for different levels of filling materials 25 %, 50 %, 75 % and 90 % in open, flat closure and cone closure silos. The first 20 modal frequencies are extracted as shown in figure. It can be seen that as the filling level is increased the frequency also increases. The less value of frequency is in open slender silo.

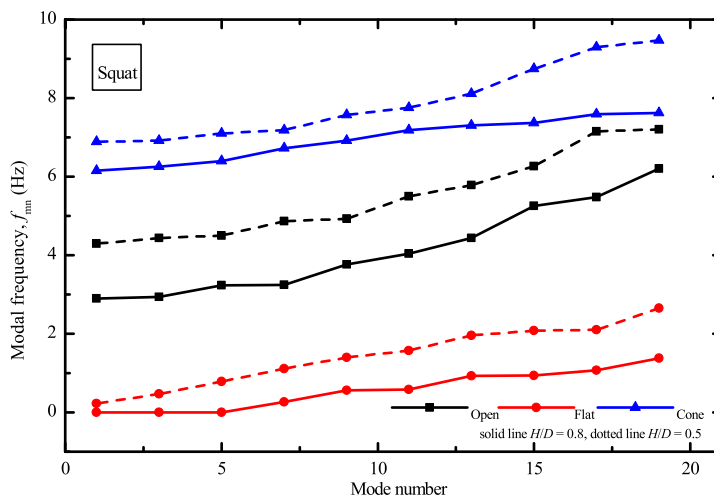
Fig. 8 shows the modal frequencies in open silo for filling materials 90 % for different aspect ratios. Thus, in case of squat silo having



(a) for  $H/D = 2.5$  and  $2.0$



(b) for  $H/D = 1.5$  and  $1.25$



(c) for  $H/D = 0.8$  and  $0.5$

**Fig. 6.** Modal frequencies in empty slender, intermediate slender and squat silos.

**Table 5**  
Modal frequencies (in Hz) in empty slender silos (S).

Type of closure	$H = 25 \text{ m}, D = 10 \text{ m}, h = 10 \text{ mm}, h_c = 10 \text{ mm}, H/D = 2.5, R/h = 500$		$H = 20 \text{ m}, D = 10 \text{ m}, h = 5 \text{ mm}, h_c = 10 \text{ mm}, H/D = 2, R/h = 1000$	
	Modes (m, n)	Frequency	Modes (m, n)	Frequency
Open	(1,1)	2.030	(1,1)	1.855
	(1,2)	2.501	(1,2)	2.044
	(1,3)	2.574	(1,3)	2.275
	(1,5)	3.623	(1,5)	2.595
	(1,6)	4.992	(1,6)	3.682
Flat	(1,1)	1.010	(1,1)	0.506
	(1,3)	2.159	(1,3)	1.073
	(1,4)	5.926	(1,4)	4.142
	(1,6)	6.741	(1,6)	4.548
	(1,7)	6.852	(1,7)	4.570
Cone	(1,1)	4.511	(1,1)	4.014
	(1,3)	5.404	(1,3)	4.538
	(1,4)	6.852	(1,4)	5.674
	(2,4)	8.707	(2,4)	6.873
	(2,6)	9.174	(2,6)	7.563

**Table 6**  
Modal frequencies (in Hz) in empty intermediate slender silos (I).


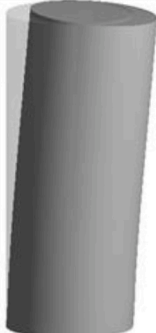
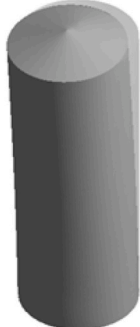
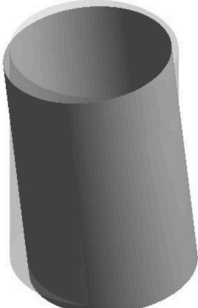
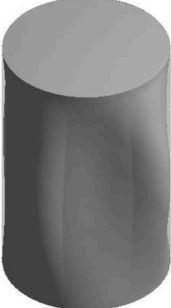
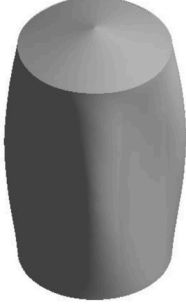
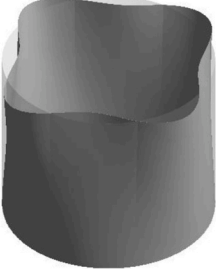
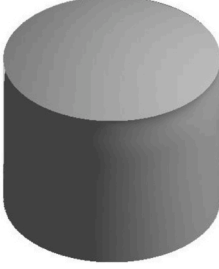
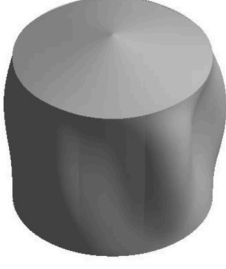
Type of closure	$H = 18 \text{ m}, D = 12 \text{ m}, h = 8 \text{ mm}, h_c = 8 \text{ mm}, H/D = 1.5, R/h = 750$		$H = 15 \text{ m}, D = 12 \text{ m}, h = 5 \text{ mm}, h_c = 5 \text{ mm}, H/D = 1.25, R/h = 1200$	
	Modes (m, n)	Frequency	Modes (m, n)	Frequency
Open	(1,1)	2.465	(1,1)	2.330
	(1,3)	2.975	(1,3)	2.427
	(1,4)	3.238	(1,4)	2.608
	(2,1)	3.786	(2,1)	3.056
	(2,3)	4.820	(2,3)	3.847
Flat	(2,1)	0.559	(2,1)	0.350
	(2,2)	1.956	(2,2)	1.241
	(2,4)	4.082	(2,4)	2.578
	(2,5)	5.165	(2,5)	3.367
	(2,6)	5.460	(2,6)	5.053
Cone	(2,1)	5.152	(2,1)	5.048
	(2,2)	5.322	(2,2)	5.061
	(2,4)	6.278	(2,4)	6.219
	(2,5)	7.772	(2,5)	7.220
	(2,6)	9.307	(2,6)	8.269

**Table 7**  
Modal frequencies (in Hz) in empty squat silos (Q).

Type of closure	$H = 12 \text{ m}, D = 15 \text{ m}, h = 6 \text{ mm}, h_c = 6 \text{ mm}, H/D = 0.8, R/h = 1250$		$H = 7.5 \text{ m}, D = 15 \text{ m}, h = 5 \text{ mm}, h_c = 5 \text{ mm}, H/D = 0.5, R/h = 1500$	
	Modes (m, n)	Frequency	Modes (m, n)	Frequency
Open	(1,4)	2.902	(1,4)	4.295
	(1,5)	3.234	(1,5)	4.441
	(1,6)	4.036	(1,6)	5.498
	(2,4)	5.254	(2,4)	6.270
	(2,6)	5.480	(2,6)	7.174
Flat	(1,1)	0.000	(1,1)	0.224
	(1,2)	0.301	(1,2)	0.776
	(1,4)	0.577	(1,4)	1.113
	(1,3)	0.940	(1,3)	1.957
	(1,5)	1.121	(1,5)	2.087
Cone	(2,1)	6.155	(2,1)	6.886
	(2,3)	6.271	(2,3)	6.974
	(2,4)	6.721	(2,4)	7.574
	(2,6)	7.179	(2,6)	8.113
	(2,5)	7.597	(2,5)	9.239

aspect ratio 0.5 the fundamental frequency is 259.26 Hz maximum. For slender 2.5, 2.0 and intermediate slender 1.5, 1.25 open silos the variation in modal frequency are in close proximity, thus corresponds to the better performance of the open silos for 90 % filling. [Table 9](#) explores the fundamental frequencies in cone silo for different levels of filling materials. With increase in the aspect ratio in

**Table 8**  
Empty silos fundamental frequencies.

Type of silo	Open	Flat	Cone
Slender ( $H/D = 2.5$ )	 2.03 Hz	 1.01 Hz	 4.51 Hz
Intermediate slender ( $H/D = 1.5$ )	 2.46 Hz	 0.55 Hz	 5.15 Hz
Squat ( $H/D = 0.8$ )	 2.90 Hz	 0.00 Hz	 6.15 Hz

cone closure the frequency decreases and further indicating that filling levels increases the mass in the silo, hence increases the frequency. From the results during the filling and emptying the silos considering the on floor practical conditions, the 75 %–90 % filling levels the variation in fundamental frequency is almost negligible. In Table 10 the tenth modal frequencies in cone silo for different levels of filling materials are discussed. To show the higher mode shapes tenth mode shapes are shown.

Table 11 gives the fundamental frequencies in open silo for different levels of filling materials. It is seen that for 90 % filling material the fundamental mode is (1, 1) for 2.0, 1.5 and 0.5 aspect ratios. In all cases the axial mode is one for the fundamental frequency. Table 12 explores the fundamental frequencies for  $H/D = 2.0$  for 90 % filling materials. It can be seen that in case of flat closure the variation in fundamental frequency in slender silo is not so much affected by the different filling levels. And same nature of results is observed in case of intermediate and squat silos also.

## 6. Regression approach for predicting mode frequency

In order to estimation the mode frequency corresponding to aspect ratio of silo, regression approach based on polynomial regression is used for predicting the mode frequency of empty and 90 % filled silos. Based on the simulated result for aspect ratio 0.5, 0.8, 1.25, 1.5, 2.0 and 2.5 and corresponding modal frequency for empty and 90 % filled silos, the polynomial relationship is

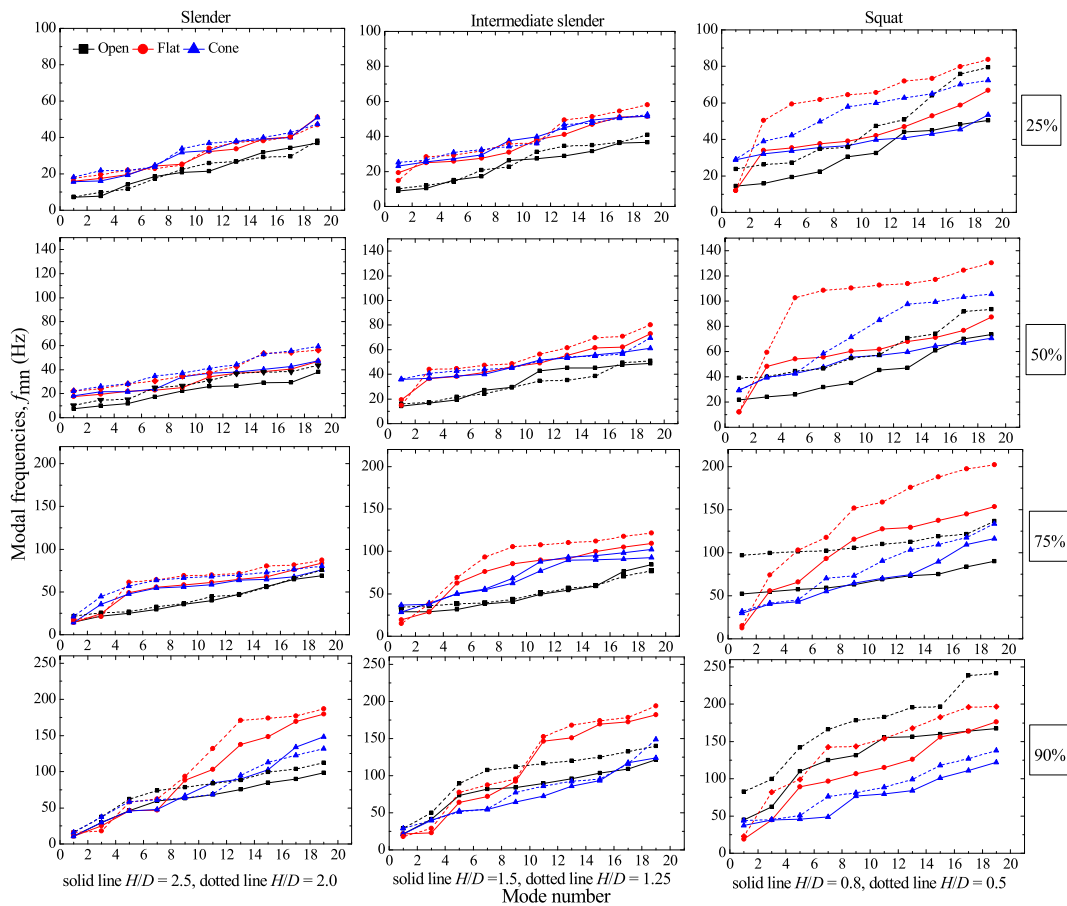


Fig. 7. Modal frequencies for different levels of filling materials.

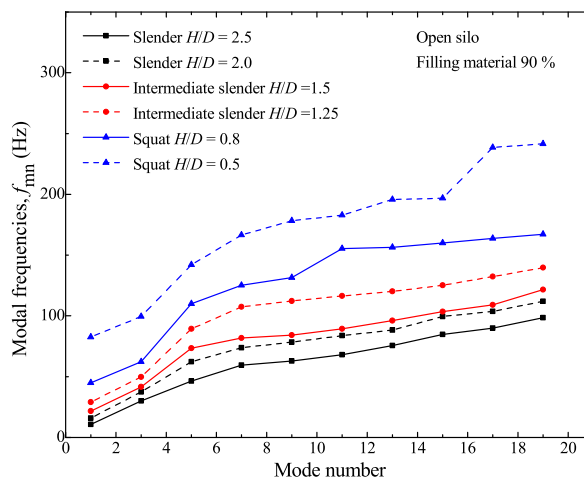


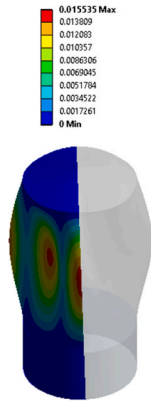
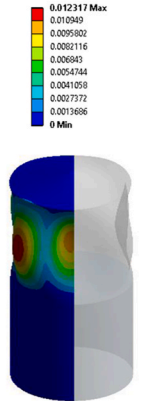
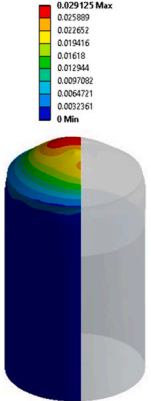
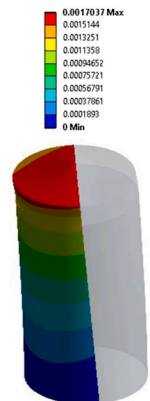
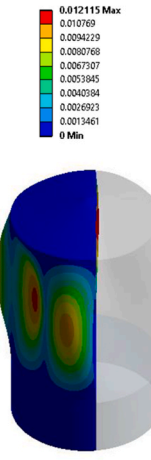
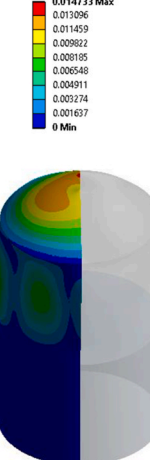
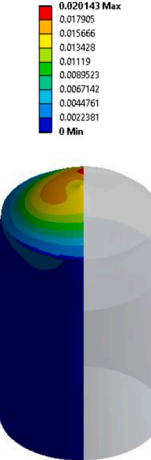
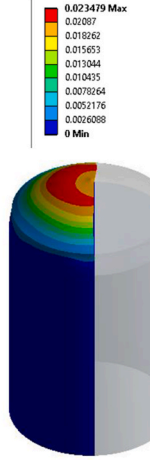
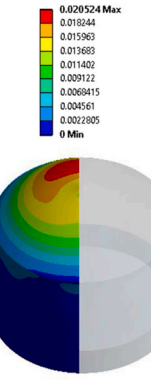
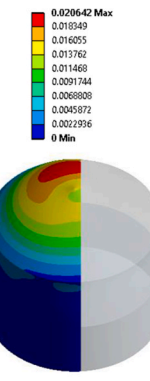
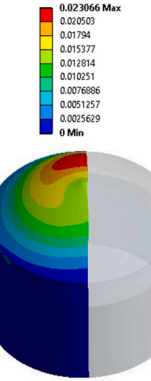
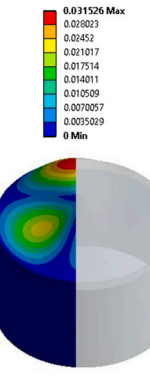
Fig. 8. Modal frequencies in open silo for filling materials 90 % for different aspect ratios.

developed. For this the first, second, third and fourth order degree polynomial regression equations are used as given in Tables 13 and 14. The generalized polynomial nth order equation is represented as,

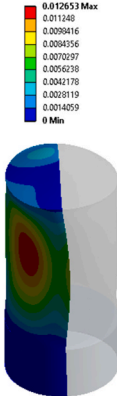
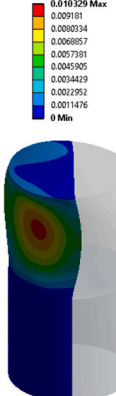
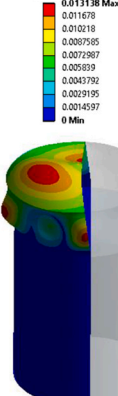
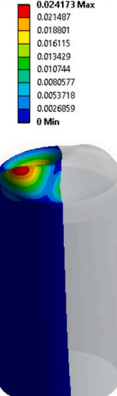
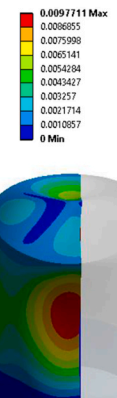
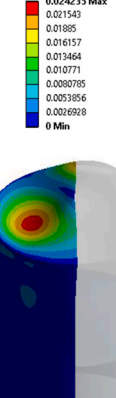
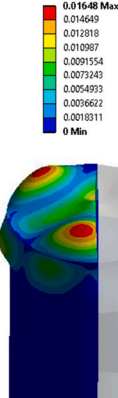
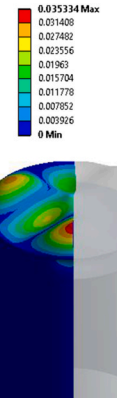
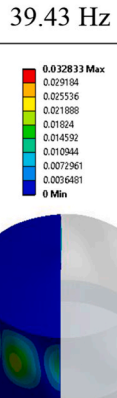
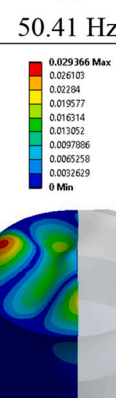
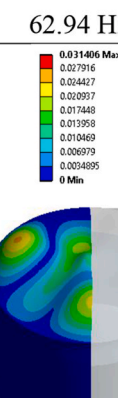
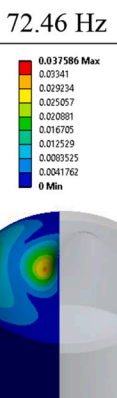
$$y(x) = (p_1 \times x^n) + (p_2 \times x^{n-1}) + \dots + (p_n \times x) + p_{n+1} \tag{12}$$

From the polynomial regression the polynomial coefficients estimated for the first, second, third and fourth order equations are

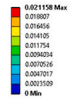
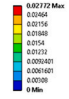
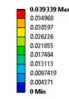
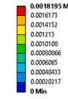
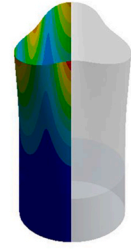
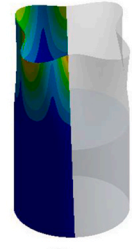
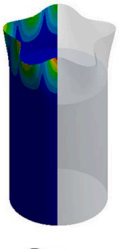
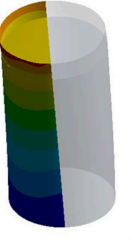
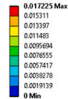
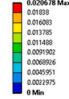
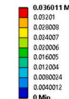
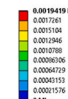
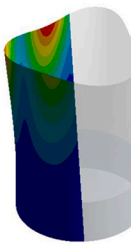
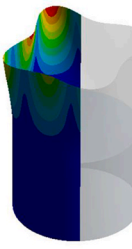



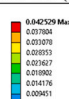
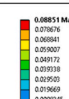
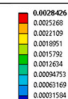
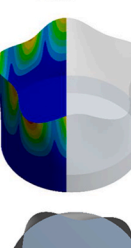

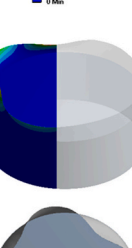

**Table 9**  
Fundamental frequencies in cone silo for different levels of filling material.

Types of silo	Different levels of filling materials			
	25%	50%	75%	90%
Slender ( $H/D = 2.0$ )	 <p>0.015535 Max 0.013809 0.012083 0.010357 0.0086306 0.0069045 0.0051784 0.0034522 0.0017261 0 Min</p> <p>18.20 Hz</p>	 <p>0.012317 Max 0.010949 0.0095802 0.0082116 0.006843 0.0054744 0.0041058 0.0027372 0.0013686 0 Min</p> <p>29.77 Hz</p>	 <p>0.029125 Max 0.025989 0.022852 0.019416 0.01618 0.012944 0.0097082 0.0064721 0.0032361 0 Min</p> <p>21.41 Hz.</p>	 <p>0.0017037 Max 0.0015144 0.0013251 0.0011358 0.00094652 0.00075721 0.00056791 0.00037861 0.0001893 0 Min</p> <p>15.78 Hz</p>
Intermediat e ( $H/D = 1.5$ )	 <p>0.012115 Max 0.010769 0.0094229 0.0080768 0.0067307 0.0053845 0.0040384 0.0026923 0.0013461 0 Min</p> <p>23.16 Hz</p>	 <p>0.014733 Max 0.013096 0.011459 0.009822 0.008185 0.006548 0.004911 0.003274 0.001637 0 Min</p> <p>35.82 Hz</p>	 <p>0.020143 Max 0.017905 0.015666 0.013428 0.01119 0.0089523 0.0067142 0.0044761 0.0022381 0 Min</p> <p>28.36 Hz</p>	 <p>0.023479 Max 0.02087 0.018262 0.015653 0.013044 0.010435 0.0078264 0.0052176 0.0026088 0 Min</p> <p>21.50 Hz</p>
Squat ( $H/D = 0.5$ )	 <p>0.020524 Max 0.018244 0.015963 0.013683 0.011402 0.009122 0.0068415 0.004561 0.0022805 0 Min</p> <p>29.14 Hz</p>	 <p>0.020642 Max 0.018349 0.016055 0.013762 0.011468 0.0091744 0.0068803 0.0045872 0.0022936 0 Min</p> <p>29.31 Hz</p>	 <p>0.023066 Max 0.020503 0.01794 0.015377 0.012814 0.010251 0.0076886 0.0051257 0.0025629 0 Min</p> <p>31.87 Hz</p>	 <p>0.031526 Max 0.028023 0.02452 0.021017 0.017514 0.014011 0.010509 0.0070057 0.0035029 0 Min</p> <p>43.58 Hz</p>

**Table 10**  
Tenth modal frequencies in cone silo for different levels of filling material.

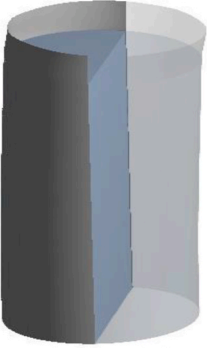
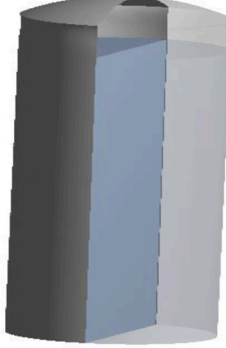
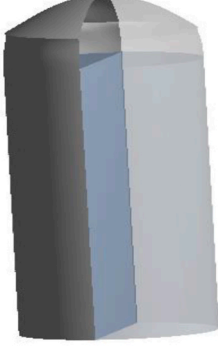
Types of silo	Different levels of filling materials			
	25%	50%	75%	90%
Slender ( $H/D = 2.0$ )	 <p>0.012653 Max 0.011246 0.009416 0.008456 0.0070297 0.0056236 0.0041178 0.0028119 0.0014059 0 Min</p> <p>33.99 Hz</p>	 <p>0.010329 Max 0.009161 0.0080334 0.006857 0.0057391 0.0045905 0.0034429 0.0022952 0.0011476 0 Min</p> <p>43.67 Hz</p>	 <p>0.013138 Max 0.011678 0.010218 0.0087585 0.0072987 0.005839 0.0043792 0.0029195 0.0014597 0 Min</p> <p>67.62 Hz</p>	 <p>0.024173 Max 0.021457 0.018801 0.016115 0.013429 0.010744 0.0080577 0.0053718 0.0026859 0 Min</p> <p>67.28 Hz</p>
Intermediate ( $H/D = 1.5$ )	 <p>0.0097711 Max 0.0086055 0.0075998 0.0065141 0.0054284 0.0043427 0.003257 0.0021714 0.0010857 0 Min</p> <p>39.43 Hz</p>	 <p>0.024235 Max 0.021543 0.01885 0.016157 0.013464 0.010771 0.0080785 0.0053856 0.0026928 0 Min</p> <p>50.41 Hz</p>	 <p>0.01648 Max 0.014649 0.012818 0.010987 0.0091554 0.0073243 0.0054933 0.0036622 0.0018311 0 Min</p> <p>62.94 Hz</p>	 <p>0.035334 Max 0.031408 0.027482 0.023556 0.01963 0.015704 0.011778 0.007852 0.003926 0 Min</p> <p>72.46 Hz</p>
Squat ( $H/D = 0.5$ )	 <p>0.032833 Max 0.029194 0.025536 0.021888 0.01824 0.014592 0.010944 0.0072961 0.0036481 0 Min</p> <p>58.94 Hz</p>	 <p>0.029366 Max 0.026103 0.02284 0.019577 0.016314 0.013052 0.0097886 0.0065258 0.0032629 0 Min</p> <p>72.28 Hz</p>	 <p>0.031406 Max 0.027916 0.024427 0.020937 0.017448 0.013958 0.010469 0.006979 0.0034895 0 Min</p> <p>75.17 Hz</p>	 <p>0.037586 Max 0.03341 0.029234 0.025057 0.020881 0.016705 0.012529 0.0083525 0.0041762 0 Min</p> <p>81.50 Hz</p>

**Table 11**  
Fundamental frequencies in open silo for different levels of filling material.

Types of silos	Different levels of filling materials			
	25%	50	75	90
Slender ( $H/D = 2.0$ )	 0.021158 Max 0.018027 0.016456 0.014105 0.011754 0.009254 0.007016 0.004767 0.002509 0 Min	 0.02772 Max 0.02464 0.02156 0.01848 0.0154 0.01232 0.0091481 0.0061401 0.003108 0 Min	 0.039339 Max 0.034968 0.030597 0.261636 0.211855 0.171884 0.131113 0.090319 0.049571 0 Min	 0.0018193 Max 0.0014773 0.001133 0.000713 0.000296 0.000066 0.000005 0.0000033 0.0000217 0 Min
	 7.27 Hz (1, 3)	 11.97 Hz (1,4)	 21.54 Hz (1, 5)	 15.82 Hz (1,1)
Intermedia ( $H/D = 1.5$ )	 0.017225 Max 0.013311 0.011387 0.011483 0.009594 0.007855 0.0057417 0.003578 0.0019139 0 Min	 0.020678 Max 0.019316 0.017395 0.015488 0.0091902 0.0068916 0.0049591 0.0023975 0 Min	 0.036011 Max 0.03101 0.026000 0.021007 0.016006 0.011005 0.011004 0.0000041 0.0000012 0 Min	 0.0019419 Max 0.001781 0.001504 0.001264 0.001088 0.000836 0.0006719 0.0004153 0.0002156 0 Min
	 9.00 Hz (1,3)	 14.10 Hz (1,4)	 28.84 Hz (1,5)	 21.66 Hz (1,1)
Squat ( $H/D = 0.5$ )	 0.020209 Max 0.01425 0.011812 0.01019 0.011915 0.011012 0.000003 0.000262 0.0010031 0 Min	 0.042529 Max 0.037804 0.031978 0.026553 0.021867 0.019082 0.014176 0.009411 0.0047255 0 Min	 0.08851 Max 0.07876 0.068841 0.059007 0.481712 0.059338 0.029509 0.019669 0.0098345 0 Min	 0.0028426 Max 0.002569 0.002109 0.001851 0.001592 0.001404 0.0009373 0.0006169 0.00031584 0 Min
	 23.70 Hz (1, 5)	 39.25 Hz (1,5)	 96.48 Hz (1,3)	 82.67 Hz (1,1)



**Table 12**  
Fundamental frequencies for  $H/D = 2.0$  for 90 % filling materials.

Open	Flat	Cone
		
15.82 Hz	15.79 Hz	15.77 Hz

**Table 13**  
Polynomial regression coefficients for empty silos.

(a) For open								
Degree	Equation	$p_1$	$p_2$	$p_3$	$p_4$	$p_5$	$R^2$	RSME
1	$p_1x + p_2$	-0.997	4.067	-	-	-	0.701	0.540
2	$p_1x^2 + p_2x + p_3$	0.919	-3.748	5.695	-	-	0.916	0.330
3	$p_1x^3 + p_2x^2 + p_3x + p_4$	-0.672	3.937	-7.71	7.134	-	0.943	0.334
4	$p_1x^4 + p_2x^3 + p_3x^2 + p_4x + p_5$	1.888	-11.968	27.281	-27.047	12.389	0.993	0.158
(b) For flat closure								
Degree	Equation	$p_1$	$p_2$	$p_3$	$p_4$	$p_5$	$R^2$	RSME
1	$p_1x + p_2$	0.415	-0.150	-	-	-	0.807	0.168
2	$p_1x^2 + p_2x + p_3$	0.155	-0.048	0.124	-	-	0.848	0.173
3	$p_1x^3 + p_2x^2 + p_3x + p_4$	-0.01	0.203	-0.112	0.147	-	0.848	0.212
4	$p_1x^4 + p_2x^3 + p_3x^2 + p_4x + p_5$	1.268	-7.596	15.879	-13.098	3.676	0.998	0.033
(c) For cone closure								
Degree	Equation	$p_1$	$p_2$	$p_3$	$p_4$	$p_5$	$R^2$	RSME
1	$p_1x + p_2$	-1.284	7.125	-	-	-	0.814	0.51
2	$p_1x^2 + p_2x + p_3$	0.866	-3.87	8.66	-	-	0.948	0.311
3	$p_1x^3 + p_2x^2 + p_3x + p_4$	0.523	-1.48	-0.789	7.538	-	0.959	0.337
4	$p_1x^4 + p_2x^3 + p_3x^2 + p_4x + p_5$	1.18	-6.57	13.19	-12.94	10.84	0.973	0.387

given in Table 13 for empty and Table 14 for 90 % filled silos. In the present work, the coefficient of determination ( $R^2$ ) and the root mean squared error (RMSE), two statistical metrics, have been used in order to verify and evaluate the created regression models. Thus, the statistical connection between two data points using the  $R^2$  value. When the linear correlation is measured, a value between 0 and 1 is obtained, with 0 denoting no correlation and 1 denoting complete correlation. The slope criterion, which is described as the slope of the linear regression fit between the predicted and observed modal frequency, is then presented. The following the algorithm for regression models used for mode frequency prediction of silo.

**Algorithm 1: Regression for Mode Frequency Prediction**

1. Model the FE model of silos ← Apply the block Lanczos method
2. Generate the frequency Vs aspect ratio features set ←  $f_{mode} @ H/D$  for closer types
3. Apply Linear regression model for initial predication ←  $f_{Linpredc} = p_1f + p_2$
4. Change the polynomial order predict the model coefficient →  $p_1, p_2 \dots, p_n$
5. Estimate the performance parameters as
 
$$RMSE = \sqrt{\frac{1}{N} \sum_{j=1}^N (y_{test}(j) - y_{predicted}(j))^2}$$
 and
 
$$R^2 = 1 - \frac{\frac{1}{N} \sum_{j=1}^N (y_{test}(j) - y_{predicted}(j))^2}{\frac{1}{N} \sum_{j=1}^N (y_{test}(j) - \overline{y_{predicted}(j)})^2}$$
6. if  $R^2 >$  criterion threshold
  - end prediction
  - else
  - Repeat 4 and 5
  - end if check
7. Use the  $n^{th}$  order polynomial solution to predict the mode frequencies. As
 
$$p(x)_n = p_1x^4 + p_2x^3 + p_3x^2 + p^4 x + p_5$$
8. Change aspect ratio and closer type and Repeat 4 to 5
9. end Algorithm

From Table 13(a) for open, Table 13(b) for flat closure and Table 13(c) for cone closure give  $R^2$  and RMSE values for first, second, third and fourth order polynomial equations. It can be observed that the best fitting for obtaining the relationship between mode frequency and aspect ratio of empty silo is by using the fourth order polynomial for open, flat and cone closure. For which the  $R^2$  is maximum and corresponding RMSE value is minimum for fourth order polynomial which is an ideal case for predicting the modal frequency for empty silo. Fig. 9 shows the predicted modal frequencies obtained for aspect ratio from 0.5 to 2.5 using fourth order polynomial regression. It can be seen that the modal frequencies is more in cone closure as compared to open and flat closure empty silos for aspect ratio 0.5 to 2.5.

Similarly, by regression approach the modal frequency is also predicted for 90 % filled silos for open, flat and cone closure. Table 14 (a) for open, Table 14(b) for flat closure and Table 14(c) for cone closure gives the polynomial coefficients estimated for the first,

**Table 14**  
Polynomial regression coefficients for 90 % filled silos.

(a) For open								
Degree	Equation	$p_1$	$p_2$	$p_3$	$p_4$	$p_5$	$R^2$	RSME
1	$p_1x + p_2$	-31.58	79.12	-	-	-	0.780	13.94
2	$p_1x^2 + p_2x + p_3$	24.79	-105.7	123	-	-	0.953	7.411
3	$p_1x^3 + p_2x^2 + p_3x + p_4$	-23.25	129.2	-242.8	172.8	-	0.988	4.436
4	$p_1x^4 + p_2x^3 + p_3x^2 + p^4 x + p_5$	23.92	-166.3	424.9	-487.7	239.4	0.997	2.789
(b) For flat closure								
Degree	Equation	$p_1$	$p_2$	$p_3$	$p_4$	$p_5$	$R^2$	RSME
1	$p_1x + p_2$	-5.09	25.23	-	-	-	0.755	2.408
2	$p_1x^2 + p_2x + p_3$	-2.716	3.03	20.42	-	-	0.833	2.298
3	$p_1x^3 + p_2x^2 + p_3x + p_4$	-5.096	20.17	-27.02	31.33	-	0.896	2.216
4	$p_1x^4 + p_2x^3 + p_3x^2 + p^4 x + p_5$	9.772	-63.56	141	-127.1	58.533	0.952	2.132
(c) For cone closure								
Degree	Equation	$p_1$	$p_2$	$p_3$	$p_4$	$p_5$	$R^2$	RSME
1	$p_1x + p_2$	-16.89	50.39	-	-	-	0.972	2.374
2	$p_1x^2 + p_2x + p_3$	4.198	-29.45	57.82	-	-	0.993	1.288
3	$p_1x^3 + p_2x^2 + p_3x + p_4$	2.163	-5.515	-16.7	53.19	-	0.995	1.394
4	$p_1x^4 + p_2x^3 + p_3x^2 + p^4 x + p_5$	-4.24	27.53	-57.94	26.72	41.39	0.996	1.702

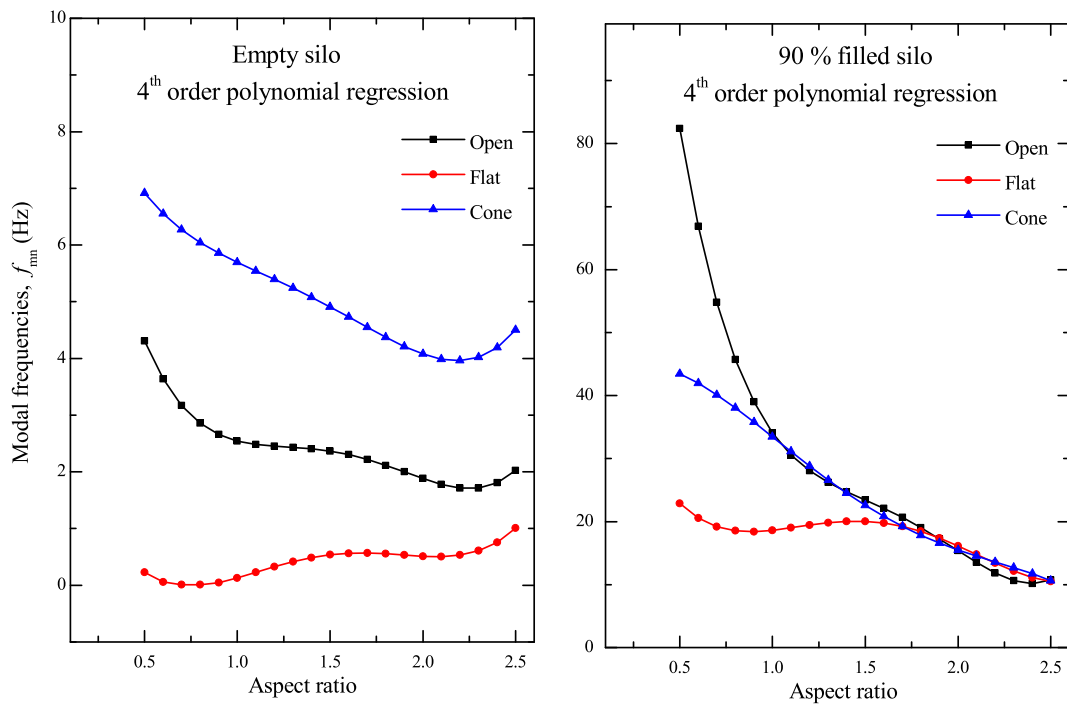


Fig. 9. 4th order polynomial regression for empty and 90 % filled silos.

second, third and fourth order polynomial equations for 90 % filled silo. In case of 90 % filled silo the best fitting for obtaining the relationship between mode frequency and aspect ratio of is obtained by the fourth order polynomial for open, flat and cone closure. For which the  $R^2$  is maximum and corresponding RMSE value is minimum for fourth order polynomial which also an ideal case for predicting the modal frequency for 90 % filled silo. Fig. 9 shows the predicted modal frequencies obtained for aspect ratio from 0.5 to 2.5 using fourth order polynomial regression. It can be seen that the modal frequencies is more in open as compared to cone and flat closure 90 % filled silos for aspect ratio up to nearly 1.5 and beyond 1.5 aspect ratio the modal frequencies are almost same for open, flat and cone silos for 90 % filled silos.

By using the regression approach based 4th order polynomial regression equations proposed in the present work will be useful in predicting the modal frequencies of empty and filled silos. In addition it is also find that for the mentioned prediction problem increasing order of polynomial beyond 4 is not feasible and degrades the efficiency. Thus, 4th order polynomial regression is selected as optimum solution.

## 7. Conclusions

In the present work the free vibration analysis of thin circular cylindrical steel silos considering various aspect ratios, slender, intermediate slender and squat silos; for empty and varying storage filled conditions is carried out. The modal frequencies for empty and 25 %, 50 %, 75 % and 90 % filled silos are evaluated. Also, silos are considered having open, flat and cone type of closures at its top, in order to study the effect of closures on the natural frequencies of silos. Finally, regression approach is adopted for predicting the mode frequency of empty and filled silos. The following conclusions are obtained from the present study.

- (1) As aspect ratio increases the fundamental frequency is reduced in empty silo. It is more in the case of squat silo. It can be seen that the fundamental frequency is less in the case of flat closure in all the aspect ratios of the silo. The frequency values are more in the case of cone closure is observed. Also as the mode number increases the modal frequency value increases.
- (2) As the filling level is increased the modal frequency also increases. The less value of frequency is in open slender silo. With increase in the aspect ratio in cone closure the frequency decreases and further indicating that filling levels increases the mass in the silo hence increases the frequency. The fundamental frequencies for  $H/D = 2.0$  for 90 % filling materials, in case of flat closure the variation in fundamental frequency in slender silo is not so much affected by the different filling levels. And same nature of results is observed in case of intermediate and squat silos also. Through these free vibration studies on empty and varying storage filled conditions of different aspect ratios will most certainly aid in comprehending the dynamic behavior of steel silos.
- (3) By using the regression approach based 4th order polynomial equations proposed in the present work will be useful in predicting the modal frequencies of empty and 90 % filled silos. The modal frequencies are more in cone closure as compared to open and flat closure empty silos for aspect ratio 0.5 to 2.5. The modal frequencies are more in open as compared to cone and

flat closure 90 % filled silos for aspect ratio up to nearly 1.5 and beyond 1.5 aspect ratio the modal frequency are almost same for open, flat and cone for 90 % filled silos.

The free vibration analysis of empty and different filled levels of silo along with different closures is examined in the present work. This investigation will definitely results in the understanding the structural and dynamic response of steel silos, also the dynamic interaction behavior between the storage materials and the structural components of flat-bottom silo.

### Additional information

No additional information is available for this paper.

### CRedit authorship contribution statement

**Aashish Kumar Jain:** Investigation, Methodology, Validation, Visualization, Writing – original draft, Funding acquisition. **Rajesh Bhargava:** Conceptualization, Writing – review & editing. **Aruna Rawat:** Conceptualization, Methodology, Writing – review & editing.

### Declaration of competing interest

The authors declare that they have no known competing financial interests or personal relationships that could have appeared to influence the work reported in this paper.

### References

- [1] P. Iwicki, J. Tejchman, J. Chroscielowski, Dynamic FE simulations of buckling process in thin-walled cylindrical metal silos, *Thin-Walled Struct.* 84 (2014) 344–359.
- [2] A.M. Mehrehtehr, S. Maleki, 3D buckling assessment of cylindrical steel silos of uniform thickness under seismic action, *Thin-Walled Struct.* 131 (2018) 654–667.
- [3] A. Dogangun, Z. Karaca, A. Durmus, H. Sezen, Cause of damage and failures in silo structures, *J. Perform. Constr. Facil.* 23 (2) (2009) 65–71.
- [4] A.J. Sadowski, J.M. Rotter, Steel silos with different aspect ratios: I – behaviour under concentric discharge, *J. Constr. Steel Res.* 67 (10) (2011) 1537–1544.
- [5] S. Silvestri, T. Trombetti, G. Gasparini, Flat-bottom grain silos under earthquake ground motion, in: *The 14th World Conference on Earthquake Engineering* October 12-17, 2008, 2008 (Beijing, China).
- [6] F. Ayuga, M. Guaíta, P. Aguado, Static and dynamic silo loads using finite element models, SE-structures and environment, *Silos research Institute* 78 (3) (2001) 299–308.
- [7] E. Gallegoa, A. Ruizb, P.J. Aguadob, Simulation of silo filling and discharge using ANSYS and comparison with experimental data, *Comput. Electron. Agric.* 118 (2015) 281–289.
- [8] V. Syamili, L. Kottalil, F.S. Thaikudiyil, Buckling analysis of thin shells, *Int. J. Civ. Eng.* 5 (1) (2016) 11–18.
- [9] L. Pieraccini, M. Palermo, S. Stefano, T. Trombetti, On the fundamental periods of vibration of flat-bottom ground supported circular silos containing gran-like material, *Procedia Eng.* 199 (2017) 248–253.
- [10] M. Hussain, M.N. Naeem, Vibration analysis of single-walled carbon nanotubes using wave propagation approach, *Mechanical Sciences* 8 (1) (2017) 155–164.
- [11] M. Hussain, M.N. Naeem, Effects of ring supports on vibration of armchair and zigzag FGM rotating carbon nanotubes using Galerkin's method, *Compos. B Eng.* 163 (2019) 548–561.
- [12] S. Mansour, Pieraccini, M. L. Palermo, D. Foti, G. Gasparini, T. Trombetti, S. Silvestri, Comprehensive review on the dynamic and seismic behavior of flat-bottom cylindrical silos filled with granular material, *Frontiers in Built Environment* 7 (2021), 805014.
- [13] P. Jiao, Z. Chen, H. Ma, P. Ge, Y. Gu, H. Miao, Buckling Behaviors of Thin-Walled Cylindrical Shells under Localized Axial Compression Loads, Part 1: Experimental Study, vol. 166, *Thin-Walled Structures*, 2021.
- [14] M. Hussain, Application of Kelvin's approach for material structure of CNT: polynomial volume fraction law. *Structural Engineering and Mechanics*, *Int. J. 76* (1) (2020) 129–139.
- [15] M. Hussain, M.N. Naeem, Mass density effect on vibration of zigzag and chiral SWCNTs, *J. Sandw. Struct. Mater.* 23 (6) (2021) 2245–2273.
- [16] M. Hussain, M.N. Naeem, Vibration characteristics of zigzag FGM single-walled carbon nanotubes based on Ritz method with ring-stiffeners, *Indian J. Phys.* 95 (2021) 2023–2034.
- [17] M. Hussain, M.N. Naeem, Rotating response on the vibrations of functionally graded zigzag and chiral single walled carbon nanotubes, *Applied Mathematical Modeling* 75 (2019) 506–520.
- [18] M. Khalil, S. Ruggieri, G. Uva, Assessment of structural behavior, vulnerability, and risk of industrial silos: state-of-the-art and recent research trends, *Appl. Sci.* 12 (3006) (2022) 1–37.
- [19] M. Hussain, FG-based computational fracture of frequency up-conversion for bistability of rotating shell: an effective numerical Scheme, *Advances in Concrete Construction, An International Journal* 13 (5) (2020) 367–376.
- [20] M. Hussain, Controlling of ring based structure of rotating FG shell: frequency distribution, *Advances in Concrete Construction, An International Journal* 14 (1) (2022) 35–43.
- [21] M. Hussain, Structural stability of laminated composite material for the effectiveness of half axial wave mode: frequency impact, *Advances in Concrete Construction An International Journal* 14 (5) (2022) 309–315.
- [22] M. Hussain, M.N. Naeem, Accurate compact solution of fluid-filled FG cylindrical tube inducting fluid term: frequency analysis, *J. Sandw. Struct. Mater.* 24 (1) (2022) 141–156.
- [23] M. Hussain, A. Selmi, Analytical vibration of FG cylindrical shell with ring support based on various configurations, *Advances in Concrete Construction An International Journal* 9 (6) (2020) 557–568.
- [24] M. Hussain, *Small-scale Computational Vibration of Carbon Nanotubes: Composite Structure*, first ed., River Publishers, Denmark, UK, 2023.
- [25] G. Almasabha, O. Alshboul, A. Shehadeh, A.S. Almuflih, Machine learning algorithm for shear strength prediction of short links for steel buildings, *Buildings* 12 (2022) 775.
- [26] Le Tien-Thinh, Practical hybrid machine learning approach for estimation of ultimate load of elliptical concrete-filled steel tubular columns under axial loading, *Adv. Civ. Eng. ume* 2020 (2020). Article ID 8832522.
- [27] M. Fransen, M. Langelaar, D.L. Schott, Application of DEM-based metamodelling in bulk handling equipment design: methodology and DEM case study, *Powder Technol.* 393 (2021) 205–218.

- [28] K. Forerg, Influence of boundary conditions on the modal characteristics of thin shells, *AIAA J.* 2 (12) (1964) 2150–2157.
- [29] C.B. Sharma, D.J. Johns, Natural frequencies of clamped-free circular cylindrical shells, *J. Sound Vib.* 21 (3) (1972) 317–318.
- [30] G.D. Galletly, J. Mistry, The free vibrations of cylindrical shells with various end closures, *Nucl. Eng. Des.* 30 (2) (1974) 249–268.
- [31] H. Chung, Free vibration analysis of circular cylindrical shells, *J. Sound Vib.* 74 (3) (1981) 331–350.
- [32] N. Ganesan, K.R. Sivasdas, Natural Frequency of cantilever circular cylindrical shells with variable thickness, *Comput. Struct.* 34 (1990) 669–671.
- [33] A. Farshidianfar, P. Oliazadeh, Free vibration analysis of circular cylindrical shells: comparison of different shell theories, *Int. J. Mech. Appl.* 2 (5) (2012) 74–80.
- [34] P.B. Ataabadi, M.R. Khedmati, M.B. Ataabadi, Free vibration analysis of orthotropic thin cylindrical shells with variable thickness by using spline functions, *Lat. Am. J. Solid. Struct.* 12 (2014) 2099–2121.
- [35] A. Rawat, V.A. Matsagar, A.K. Nagpal, Finite element analysis of thin circular cylindrical shells, *Proceeding Indian National Science Academy* 82 (2) (2016) 349–355.
- [36] B. Hu, C. Gao, H. Zhang, H. Li, F. Pang, J. Lang, Free vibration characteristics of moderately thick spherical shell with general boundary conditions based on Ritz method, *Shock Vib.* (2020) 1–20. Article ID 4130103.
- [37] R. Anwar, M. Ghamkhar, M.I. Khan, R. Safdar, M.Z. Iqbal, W. Jamshed, E.K. Akgul, M. Prakash, Frequency analysis for functionally graded material cylindrical shells: a significant case study, *Math. Probl Eng.* 2021 (2021) 1–10. Article ID 4843321.
- [38] G. Cong, P. Fuzhen, C. Jie, L. Haichao, Free and forced vibration analysis of uniform and stepped combined conical-cylindrical-spherical shells: a unified formulation, *Ocean Eng.* 260 (2022).
- [39] S.S. Rao, *Vibration of Continuous Systems*, John Wiley & Sons, Inc., Hoboken, New Jersey, 2007.
- [40] A.E.H. Love, The Small Free Vibrations and Deformation of Thin Elastic Shell, 179A, *Philosophical Transactions of the Royal Society of London*, 1888, pp. 491–546.
- [41] A.E.H. Love, *A Treatise on the Mathematical Theory of Elasticity*, fourth ed., Dover Publications, New York, NY, 1944.
- [42] A.W. Leissa, *Vibration of Shell*. NASA SP-288, U.S. Government Printing Office, Washington, DC, 1973.
- [43] P. Chen, S.L. Sun, Q.C. Zhao, Y.C. Gong, Y.Q. Chen, M.W. Yuan, Advances in solution of classical generalized eigenvalue problem, *Interact. Multiscale Mech.* 1 (2) (2008) 211–230.
- [44] K.L. Barton, D.A. Bristow, A.G. Alleyne, A numerical method for determining monotonicity and convergence rate in iterative learning control, *Int. J. Control* 83 (2) (2010) 219–226.
- [45] Ansys 12, ANSYS Inc., Canonsburg, PA, 2009.
- [46] EN, 1991-4., Eurocode 1: Basis of Design and Actions on Structures, Part 4 - Silos and Tanks, CEN, Brussels, 2007.